

MOTION SENSING BY A TWO-PROBE IMPLEMENTATION OF MICROWAVE INTERFEROMETRY

This paper addresses the possibility of displacement measurement by microwave interferometry at an unknown reflection coefficient with the use of two probes mounted in a waveguide section. The aim of this paper is to show that the displacement measurement accuracy can be improved by using an interprobe distance other than its conventional value. The case of an arbitrary interprobe distance is considered. The measurement error as a function of the interprobe distance and the reflection coefficient is analyzed with the inclusion of variations of the currents of the semiconductor detectors connected to the probes from their theoretical values. The analysis has shown that as the interprobe distance decreases, the measurement error passes through a minimum for reflection coefficients close to unity and increases monotonically for smaller reflection coefficients. This behavior of the error is due to the fact that with decreasing interprobe distance and/or reflection coefficient the inherent error of two-probe measurements decreases, while the error caused by variations of the detector currents from their theoretical values increases. The interprobe distance is suggested to be one tenth of the guided operating wavelength λ_g . In comparison with the conventional interprobe distance of $\lambda_g/8$, the suggested value offers a marked reduction in the measurement error for reflection coefficients close to unity, while for smaller ones this error increases only negligibly. This is verified by experiment using both free-space and waveguide measurements. The results reported in this paper may be used in the development of microwave displacement sensors for various classes of vibration protection and workflow control systems.

Keywords: vibration, displacement, interferometry, probe, incident wave, reflected wave, semiconductor detector, detector current.

Microwave interferometry is an ideal means for displacement measurement in various engineering applications [1]. This is due to its ability to provide fast noncontact measurements, applicability to dusty or smoky environments (as distinct from laser Doppler sensors [2 – 4] or vision-based systems using digital image processing techniques [5]), and simple hardware implementation. In microwave interferometry, the displacement of the object under measurement (target) is extracted from the phase shift between the signal reflected from the target and the reference signal. At present, this phase shift is usually determined using special hardware incorporating a power divider and a phase-detecting processor, which is an analog [6] or a digital [7] quadrature mixer. In doing so, measures have to be taken to minimize the nonlinear phase response of the quadrature mixer, which is caused by its phase and amplitude unbalances.

Earlier, a two-probe displacement measurement technique has been proposed at the Institute of Technical Mechanics of the National Academy of Sciences of Ukraine and the State Space Agency of Ukraine [8, 9]. In that technique, the quadrature signals needed for the determination of the phase shift are extracted from the outputs of two probes placed in a waveguide section one eighth of the guided operating wavelength λ_g apart. In hardware implementation, that technique is far simpler than conventional techniques based on quadrature mixing [6, 7]. Its distinctive feature is the possibility of displacement measurement at an unknown reflection coefficient with as few as two probes, while since the classic text by Tischer [10] it has been universally believed that at least three probes are needed to determine or eliminate the unknown reflection coefficient. Theoretically, that technique gives the exact value of the displacement for reflection coefficients (at the location of the probes) no greater than $1/\sqrt{2}$ and in the general case

determines it to a worst-case accuracy of about 4.4% of the operating wavelength. The aim of this paper is to show that this accuracy can be improved by using an interprobe distance other than the conventional $\lambda_g/8$. This aim is achieved by extending the approach proposed in [8, 9] to the case of an arbitrary interprobe distance.

Consider two probes, 1 and 2, with square-law semiconductor detectors placed l apart in a waveguide section between a microwave oscillator and a target so that probe 2 is closer to the target. The detector currents J_1 and J_2 (normalized to their matched-load values) are

$$J_1 = 1 + R^2 + 2R\cos\psi, \quad (1)$$

$$J_2 = 1 + R^2 + 2R\sin(\psi - \beta), \quad (2)$$

$$\psi = \frac{4\pi x}{\lambda} + \phi, \quad \beta = \frac{\pi}{2} \left(\frac{l - \lambda_g/8}{\lambda_g/8} \right)$$

where R and ψ are the magnitude and phase of the unknown complex reflection coefficient at the location of probe 1 (for simplicity, in the following discussion the magnitude of the complex reflection coefficient will be referred to as the reflection coefficient), x is the distance between the target and probe 1, λ is the free-space operating wavelength, and the term ϕ , which is governed by the waveguide section and horn antenna geometry and the phase shift caused by the reflection, does not depend on the distance x .

Let it be desired to find the displacement $\Delta x(t)$ of the target relative to its initial position $x(t_0)$ from the measured currents $J_1(t)$ and $J_2(t)$. As will be shown below, this displacement can be unambiguously determined from the quadrature signals $\cos\psi$ and $\sin\psi$. From Eqs. (1) and (2) we have

$$\cos\psi = \frac{a_1 - R^2}{2R}, \quad (3)$$

$$\sin\psi = \frac{a_2 + a_1 \sin\beta - R^2(1 + \sin\beta)}{2R\cos\beta}, \quad (4)$$

where $a_1 = J_1 - 1$, $a_2 = J_2 - 1$.

Combining the squares of Eqs. (3) and (4) gives the biquadratic equation in R

$$R^4 - [a_1 + a_2 + 2(1 - \sin\beta)] R^2 + \frac{a_1^2 + a_2^2 + 2a_1 a_2 \sin\beta}{2(1 + \sin\beta)} = 0. \quad (5)$$

This equation has two positive roots. Let R_1 and R_2 be the greater and the smaller positive root, respectively. Clearly one of the two roots is extraneous.

Using Eqs. (3) and (4), the absolute term of Eq. (5) can be brought to the form

$$\frac{\mathbf{a}_1^2 + \mathbf{a}_2^2 + 2\mathbf{a}_1\mathbf{a}_2 \sin\beta}{2(1 + \sin\beta)} = R^2 \left\{ R^2 + 2R[\cos\psi + \sin(\psi - \beta)] + 2(1 - \sin\beta) \right\}.$$

Since the absolute term of a biquadratic equation is the product of its roots, for the extraneous root R_{ext} we have

$$R_{\text{ext}} = \left\{ R^2 + 2R[\cos\psi + \sin(\psi - \beta)] + 2(1 - \sin\beta) \right\}^{1/2}. \quad (6)$$

On rearrangement, the expression for R_{ext} becomes

$$R_{\text{ext}} = \left[R^2 + 4R_0R \sin(\psi + \arcsin R_0) + 4R_0^2 \right]^{1/2}, \quad (7)$$

where $R_0 = \sqrt{(1 - \sin\beta)/2}$.

Using Eq. (7), it can be shown that R_{ext} and R are compared as follows: $R_{\text{ext}} \geq R$ for $\sin(\psi + \arcsin R_0) \geq -R_0/R$ and $R_{\text{ext}} < R$ for $\sin(\psi + \arcsin R_0) < -R_0/R$. Since by definition $R_1 \geq R_2$, for the reflection coefficient R we have

$$R = \begin{cases} R_2, & \sin(\psi + \arcsin R_0) \geq -R_0/R, \\ R_1, & \sin(\psi + \arcsin R_0) < -R_0/R. \end{cases}$$

First consider the case $R \leq R_0$. In this case the condition $\sin(\psi + \arcsin R_0) \geq -R_0/R$ is met at any ψ , and thus the reflection coefficient R is unambiguously determined from Eq. (5) as its root R_2 , thus allowing $\cos\psi$ and $\sin\psi$ to be unambiguously determined from Eqs. (3) and (4). Given $\cos\psi$ and $\sin\psi$, the target displacement can be extracted using the phase unwrapping method, which is a powerful tool to resolve the phase ambiguity problem in a number of applications [11, 12]. The displacement Δx of the target at time t_n , $n = 0, 1, 2, \dots$, from its initial position $x(t_0)$ can be found by the following phase unwrapping algorithm [13]

$$\varphi(t_n) = \begin{cases} \arctan \frac{\sin\psi(t_n)}{\cos\psi(t_n)}, & \sin\psi(t_n) \geq 0, \cos\psi(t_n) \geq 0, \\ \arctan \frac{\sin\psi(t_n)}{\cos\psi(t_n)} + \pi, & \cos\psi(t_n) < 0, \\ \arctan \frac{\sin\psi(t_n)}{\cos\psi(t_n)} + 2\pi, & \sin\psi(t_n) < 0, \cos\psi(t_n) \geq 0, \end{cases} \quad (8)$$

$$\Delta\varphi(t_n) = \varphi(t_n) - \varphi(t_{n-1}), \quad (9)$$

$$\theta(t_n) = \begin{cases} 0, & n = 0, \\ \theta(t_{n-1}) + \Delta\varphi(t_n), & |\Delta\varphi(t_n)| \leq \pi, \quad n = 1, 2, \dots, \\ \theta(t_{n-1}) + \Delta\varphi(t_n) - 2\pi \operatorname{sgn}[\Delta\varphi(t_n)], & |\Delta\varphi(t_n)| > \pi, \quad n = 1, 2, \dots, \end{cases} \quad (10)$$

$$\Delta x(t_n) = \frac{\lambda}{4\pi} \theta(t_n), \quad n = 0, 1, 2, \dots, \quad (11)$$

where φ and θ are the wrapped and the unwrapped phase, respectively.

In the case $R > R_0$, the root R_2 will not always be equal to R , but, as will be shown below, the displacement can also be determined to sufficient accuracy assuming that $R = R_2$. As shown above, the root R_2 is extraneous if $\sin(\psi + \arcsin R_0) < -R_0/R$. In terms of the wrapped phase φ , this condition becomes

$$\varphi_1 < \varphi < \varphi_2,$$

where

$$\varphi_1 = \pi + \arcsin \frac{R_0}{R} - \arcsin R_0, \quad \varphi_2 = 2\pi - \arcsin \frac{R_0}{R} - \arcsin R_0.$$

In the case $l \leq \lambda_g/8$ ($1/\sqrt{2} \leq R_0 < 1$), we have

$$\frac{\pi}{4} \leq \arcsin R_0 \leq \arcsin \frac{R_0}{R} < \frac{\pi}{2},$$

whence it follows that the angles φ_1 and φ_2 are in the third quadrant.

If the extraneous root R_{ext} is taken as the reflection coefficient, Eqs. (3) and (4) for $\cos \psi$ and $\sin \psi$ will give their apparent values, for which in view of Eqs. (6) and (7) we will have

$$\cos \psi_{\text{ap}} = -\frac{1 + R \sin(\varphi - \beta) - \sin \beta}{R_{\text{ext}}},$$

$$\sin \psi_{\text{ap}} = -\frac{1 + R \cos \varphi - \sin \beta [\sin \beta - R \sin(\varphi - \beta)]}{R_{\text{ext}} \cos \beta}.$$

Eq. (8) for the determination of the wrapped phase includes the inverse tangent of the ratio $\sin \psi / \cos \psi$. So consider the function $F(\varphi) = \sin \psi_{\text{ap}} / \cos \psi_{\text{ap}}$, $\varphi_1 < \varphi < \varphi_2$

$$F(\varphi) = \frac{1 + R \cos \varphi - \sin \beta [\sin \beta - R \sin(\varphi - \beta)]}{\cos \beta [1 + R \sin(\varphi - \beta) - \sin \beta]}.$$

For its derivative with respect to φ we have

$$F'(\varphi) = \frac{R^2 \left[-2 \frac{R_0}{R} \sin(\varphi + \arcsin R_0) - 1 \right]}{[1 + R \sin(\varphi - \beta) - \sin \beta]^2} > \frac{R^2 [2R_0^2 - 1]}{[1 + R \sin(\varphi - \beta) - \sin \beta]^2} \geq 0.$$

Thus the apparent wrapped phase φ_{ap} is a steadily increasing function of the actual wrapped phase φ . Since at the points $\varphi = \varphi_1$ and $\varphi = \varphi_2$ the apparent and the actual phase coincide, this means that the actual phase is also between φ_1 and φ_2 , i. e. in the third quadrant. Thus the phase error $\Delta\varphi_{er} = \varphi_{ap} - \varphi$ is

$$\Delta\varphi_{er}(\varphi) = \begin{cases} 0, & 0 \leq \varphi \leq \varphi_1, \varphi_2 \leq \varphi \leq 2\pi \\ \arctan F(\varphi) + \pi - \varphi, & \varphi_1 < \varphi < \varphi_2 \end{cases} \quad (12)$$

As can be seen from Eqs. (9) – (11), the displacement error is governed only by the phase error at the initial and the current measurement point because the intermediate points cancel one another. Because of this, the maximum displacement error will be

$$\Delta x_{er \max} = \frac{\lambda}{4\pi} (\Delta\varphi_{er \max} - \Delta\varphi_{er \min}), \quad (13)$$

where $\Delta\varphi_{er \max}$ and $\Delta\varphi_{er \min}$ are the maximum and the minimum value of the function $\Delta\varphi_{er}(\varphi)$ on the interval $0 \leq \varphi < 2\pi$.

A straightforward calculation by Eqs. (12) and (13) shows that the error $\Delta x_{er \max}$ decreases rapidly with decreasing interprobe distance. However, in actual practice the interprobe distance cannot be decreased below a certain lower limit. The fact is that with decreasing interprobe distance the detector currents approach each other, thus increasing the contribution of the error component caused by variations of the detector currents from their theoretical values given by Eqs. (1) and (2) (such variations may be due to the effect of the reflecting surface shape and orientation and the antenna radiation pattern on the reflected wave, electromagnetic noise, etc.). As a result, at some value of the interprobe distance the error may pass through a minimum and start increasing.

Calculations were conducted to find out an advisable value of the interprobe distance. In the calculations, the determination of the relative displacement of a target executing a harmonic vibratory motion was simulated. In doing so, variations of the detector currents from their theoretical values were modeled by random current noise. The distance x of the target to probe 1 and the detector currents J_1 and J_2 were simulated as

$$x(t) = x_0 + A \sin(2\pi t/T),$$

$$\psi = \psi_0 + \frac{4\pi}{\lambda} A \sin(2\pi t/T), \quad \psi_0 = \phi + \frac{4\pi x_0}{\lambda},$$

$$J_1 = (1 + R^2 + 2R\cos\psi)(1 + A_n r),$$

$$J_2 = [1 + R^2 + 2R\sin(\psi - \beta)](1 + A_n r)$$

where t is the time, A and T are the target vibration amplitude and period, x_0 and ψ_0 are the distance x and the phase ψ at $t = 0$, A_n is the noise amplitude, and r is a random variable uniformly distributed between -1 and 1 .

The calculations were conducted for different values of the interprobe distance l and the reflection coefficient R at $A = 2.5\lambda$ $A_n = 0.03$. To get the maximum possible error, the initial phase ψ_0 was chosen such that $\Delta\varphi_{er}(\psi_0) = \Delta\varphi_{er\min}$.

Fig. 1 shows the ratio $\Delta x_{er\max}(\lambda_g/8)/\Delta x_{er\max}(l)$ for five cycles of vibration versus the interprobe distance l at different values of the reflection coefficient R . As illustrated, with decreasing interprobe distance this ratio passes through a maximum (i. e. the error $\Delta x_{er\max}$ passes through a minimum) for reflection coefficients close to unity ($R = 1; 0,95; 0,9$) and decreases monotonically (i. e. the error $\Delta x_{er\max}$ monotonically increases) for smaller reflection coefficients ($R = 0,7; 0,3; 0,2; 0,1$). The nonmonotonicity of the error has been discussed above. Its monotonic increase is due to the fact that for $R < R_0$ (for $l \leq \lambda_g/8$ $R_{0\min} = 1/\sqrt{2} = 0,707$) the displacement error is governed only by variations of the detector currents from their theoretical values. As can be seen from the figure, $l = 0,8(\lambda_g/8) = \lambda_g/10$ may be chosen as an advisable interprobe distance because at this value of l , in comparison with $l = \lambda_g/8$, the error shows a more than two-fold decrease for reflection coefficients close to unity while remaining much the same for smaller ones.

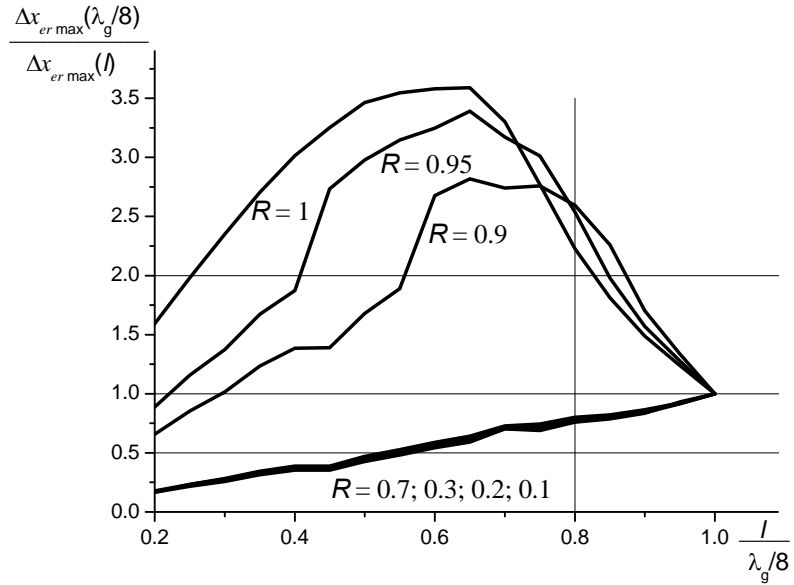


Fig. 1

In the experimental verification of the proposed technique, the two-probe measuring setup described in [8] was used. To cover the cases of both small and near-unity reflection coefficients, free-space and waveguide measurements were made. In the experiments, the interprobe distance remained fixed, and the ratio l/λ_g was varied by varying the microwave oscillator frequency. Two frequencies were used: 9.7 GHz ($l = \lambda_g/8$) and 8.7 GHz ($l = \lambda_g/10$). The reflection coefficient was determined from Eq. (5) as its root R_2 .

In the free-space measurements, the target was a $\varnothing 218$ mm brass disc put in motion by an electrically driven crank mechanism. The disc peak-to-peak amplitude was 10 cm, and the minimum distance between the disc and the antenna was 58 cm. At 9.7 GHz ($l = \lambda_g/8$) and 8.7 GHz ($l = \lambda_g/10$), the measured reflection coefficient varied between 0.16 and 0.25 and between 0.18 and 0.33, respectively, i. e. in both cases it was smaller than $R_{0\min} = 1/\sqrt{2} = 0.707$, and thus the root R_2 gave the actual reflection coefficient. For seven successive full travels of the disk, the peak-to-peak amplitude error was 0.23, 0.23, 0.18, 0.18, 0.18, 0.18 and 0.19 mm at 9.7 GHz ($l = \lambda_g/8$) and 0.35, 0.39, 0.39, 0.39, 0.39, 0.39, and 0.35 mm at 8.7 GHz ($l = \lambda_g/10$). Thus for these small values of the reflection coefficient the peak-to-peak amplitude measurement error at 8.7 GHz ($l = \lambda_g/10$) does not increase much in comparison with 9.7 GHz ($l = \lambda_g/8$).

In the waveguide measurements, a short-circuiting piston was mounted at the end of the waveguide section with the probes in place of the horn antenna used in the free-space measurements. The displacement was measured as the piston was moved every 1 mm (in the piston displacement determination, the guided wavelength λ_g was used in Eq. (11) in place of the free-space wavelength λ). Fig. 2 shows the displacement measurement error Δx_{er} (a) and the measured reflection coefficient R_2 versus the piston displacement Δx for 9.7 GHz ($l = \lambda_g/8$) and 8.7 GHz ($l = \lambda_g/10$). The measured reflection coefficient shows near-unity plateaus and valleys. The plateaus correspond to the actual reflection coefficient, and the valleys occur where the root R_2 becomes extraneous, which also manifests itself as the increase in the displacement error observed at the location of the valleys. As follows from Eq. (7), the extraneous root reaches its minimum at $\sin(\psi + \arcsin R_0) = -1$, and this minimum is

$$R_{\text{ext min}} = |R - 2R_0|.$$

At $l = \lambda_g/8$, $R_0 = 1/\sqrt{2}$ and $R_{\text{ext min}} = |R - 2R_0| = 2\sqrt{2} - 1 = 0.41$. At $l = \lambda_g/10$, $R_0 = \sqrt{(1 + \sin 0.1\pi)}/2 = 0.81$ and $R_{\text{ext min}} = |R - 2R_0| = 2 \cdot 0.81 - 1 = 0.62$. The measured values of $R_{\text{ext min}}$ at $l = \lambda_g/8$ and $l = \lambda_g/10$ are 0.28 and 0.57, respectively, i. e. they are in satisfactory agreement with the calculated ones.

As can be seen from the figure, the maximum displacement error decreases from 1.8 mm at $l = \lambda_g/8$ (4.3% of $\lambda_g = 4.18$ cm) to 0.6 mm at $l = \lambda_g/10$ (1.2%

of $\lambda_g = 5.21$ cm). The decrease in the displacement error in this case (a near-unity reflection coefficient) is much greater than its increase in the case of a small reflection coefficient discussed above.

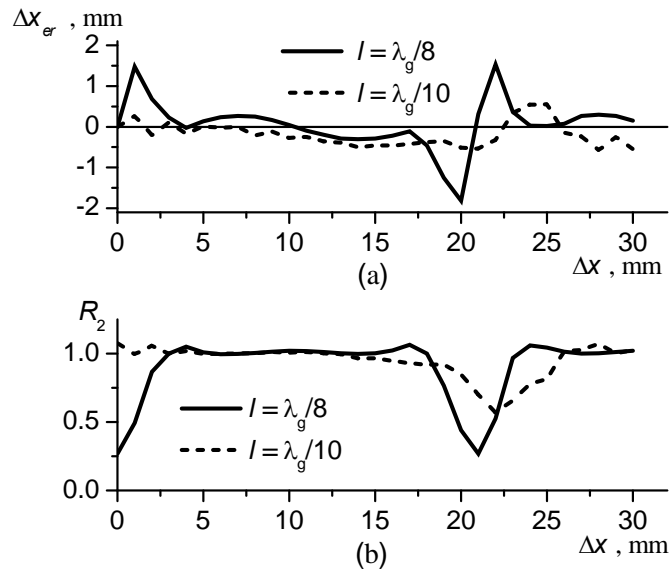


Fig. 2

Thus when measuring the displacement of a target with an unknown reflection coefficient by microwave interferometry with the use of two probes, the measurement error can be reduced by going from the conventional interprobe distance of $\lambda_g/8$ to $\lambda_g/10$. The proposed technique may be used in the development of microwave displacement sensors for various classes of vibration protection and workflow control systems.

1. Viktorov V. A. Radiowave Measurements of Process Parameters (in Russian) / V. A. Viktorov, B. V. Lunkin, A. S. Sovlukov – Moscow: Energoatomizdat, 1989. – 208 p.
2. Cunha A. Dynamic measurements on stay cables of stay-cable bridges using an interferometry laser system / A. Cunha, E. Caetano // Experimental Techniques. – 1999. – V. 23, No 3. – P. 38 – 43.
3. Kaito K. Development of a non-contact scanning vibration measurement system for real-scale structures / K. Kaito, M. Abe, Y. Fujino // Structure and Infrastructure Engineering. – 2005. – V. 1, No 3. – P. 189 – 205.
4. Mehrabi A. B. In-service evaluation of cable-stayed bridges, overview of available methods, and findings / A. B. Mehrabi // Journal of Bridge Engineering. – 2006. – V. 11, No 6. – P. 716 – 724.
5. Lee J. J. A vision-based system for remote sensing of bridge displacement / J. J. Lee, M. Shinozuka // NDT & E International. – 2006. – V. 39, No 5. – P. 425 – 431.
6. Kim S. A displacement measurement technique using millimeter-wave interferometry / S. Kim, C. Nguyen // IEEE Transactions on Microwave Theory and Techniques. – 2003. – Vol. 51, No. 6. – P. 1724 – 1728.
7. Kim S. On the development of a multifunction millimeter-wave sensor for displacement sensing and low-velocity measurement / S. Kim, C. Nguyen // IEEE Transactions on Microwave Theory and Techniques. – 2004. – V. 52, No 11. – P. 2503 – 2512.
8. Two-probe implementation of mechanical motion sensing by microwave interferometry (in Russian) / O. V. Pylypenko, N. B. Gorev, A. V. Doronin, I. F. Kodzheshpurova, E. N. Privalov // Tekhnicheskaya Mekhanika – 2013. – No 4. – P. 112 – 122.
9. Patent for Utility Model No 80300 Ukraine, IPC G01H 9/00. Motion and Vibration Sensing Method (in Ukrainian) / Pylypenko O. V., Gorev M. B., Doronin O. V., Kodzheshpurova I. F., Privalov E. M. ; applicant and patentee the Institute of Technical Mechanics of the National Academy of Sciences of Ukraine and the National Space Agency of Ukraine. – u 2012 12694 ; filed 07.11.2012 ; published 27.05.2013, Bulletin No 10. – 8 p.
10. Tischer F. J. Mikrowellen-Messtechnik / F. J. Tischer – Berlin : Springer-Verlag, 1958. – 368 p.

11. *Chavez S.* Understanding phase maps in MRI: A new cutline phase unwrapping method / *S. Chavez, Q.-S. Xiang, L. An* // IEEE Transactions on Medical Imaging. – 2002. – V. 21, No 8. – P. 966 – 977.
12. Resolving phase ambiguity in the inverse problem of reflection-only measurement methods / *U. S. Hasar, J. J. Barroso, C. Sabah, Y. Kaya* // Progress in Electromagnetics Research. – 2012. – V. 129. – P. 405 – 420.
13. *Silvia M. T.* Deconvolution of Geophysical Time Series in the Exploration for oil and Natural Gas / *M. T. Silvia, E. A. Robinson.* – Amsterdam – Oxford – New York : Elsevier Scientific Publishing Company, 1979. – 447 p.

Institute of Technical Mechanics of the National
Academy of Sciences of Ukraine and the State
Space Agency of Ukraine

Received 10.11.14,
in final form 10.11.14.